
*Research article***Adaptive and predictive controllers applied to onshore wind energy conversion system****Carla Viveiros^{1,4}, Rui Melicio^{1,2,3,*}, Victor Mendes^{2,4,5} and Jose Igreja^{4,6}**¹ ICT, Universidade de Évora, Évora, Portugal² Departamento de Física, Escola de Ciências e Tecnologia, Universidade de Évora, Portugal³ IDMEC, Instituto Superior Técnico, Universidade de Lisboa, Lisboa, Portugal⁴ Instituto Superior de Engenharia de Lisboa, Lisboa, Portugal⁵ CISE, Electromechatronic Systems Research Centre, Universidade da Beira Interior, Portugal⁶ INESC-ID, Lisboa, Portugal*** Correspondence:** Email: ruimelicio@gmail.pt; Tel: +351968547437.

Abstract: This paper presents a simulation of onshore energy conversion system connected to the electric grid and under an event-based supervisor control based on deterministic version of a finite state machine. The onshore energy conversion system is composed by a variable speed wind turbine, a mechanical transmission system described by a two-mass drive train, a gearbox, a doubly fed induction generator rotor and by a two-level converter. First, mathematical models of a variable speed wind turbine with pitch control are studied, followed by the study of different controller types such as adaptive controllers and predictive controllers. The study of an event-based supervisor based on finite state machines is also studied. The control and supervision strategy proposed for the onshore energy conversion system is based on a hierarchical structure with two levels, execution level where the adaptive and predictive controllers are included, and the supervision level where the event-based supervisor is included. The objective is to control the electric output power around the reference power and also to analyze the operational states according to the wind speed. The studied mathematical models are integrated into computer simulations for the onshore energy conversion system and the obtained numerical results allow for the performance assessment of the system connected to the electric grid. A comparison of the onshore energy conversion system performance without or with the supervisor is carried out to assess the influence of the control and supervision strategy on the performance.

Keywords: adaptive control; model predictive control; wind energy; event-based supervisor; performance assessment; onshore; finite state machine

1. Introduction

The increase in the use of renewable energy sources combined with energy efficiency measures has reduced consumption and imports of fossil fuels and has consequently contributed to increase the representativeness of renewable energies in final energy consumption. The overall capacity of all wind turbines installed worldwide by the end of 2017 reached 539 GW [1]. The annual onshore and offshore wind installations achieved, respectively, 12.5 GW and 3.1 GW in EU. There are differences between onshore and offshore exploitation of wind energy, mostly due to the: the wind speed is relatively more stable at offshore than at onshore; the wind speed at offshore is about 20% higher than at onshore. Both these differences imply that the utilization rate is higher at offshore than at onshore. Economically wind energy conversion systems at offshore tend to have larger capacity and benefit from larger areas than the limited and mostly occupied areas at onshore. But, some issues must be regarded with caution, for instance, regarding preservation of fishing, boat navigation, ocean habitat and species, marine conservation zone, landscape view from land to sea and vice versa. Higher reliability, resistant to corrosion due to the difficulties and costs of maintenance or repairing at offshore and consideration of action of sea waves on wind energy conversion systems are needed. Turbines need to be designed to take advantage of the higher level of the wind speed, i.e., the design must consider a higher value for the cut-out wind speed: the wind speed at which the wind turbine shuts down to prevent mechanical damage of the structure. Foundations work at offshore are more expensive, than on onshore where the process uses either rods drilled into the ground or a reinforced concrete pad set in the ground. Turbines need to be designed to take advantage of the higher level of the wind speed at offshore, i.e., the design must consider a higher value for the cut-out wind speed: The wind speed at which the wind turbine shuts down to prevent mechanical damage of the structure. Foundations work at offshore are more expensive, than on onshore where the process uses either rods drilled into the ground or a reinforced concrete pad set in the ground.

The technology applied on wind energy conversion systems having variable-speed and variable-pitch (VSVP) has been reported in literature due to advantageous energy capturing [2,3]. Also, amongst the electrical generators available for equipping wind turbines having VSVP, doubly-fed induction generator (DFIG) stands out in industry and became the mainstream choice [4,5].

Control system architectures are necessary to improve the quality of electrical energy delivered into the electric grid. Pitch control is widely used to ensure the best performance during the capture of energy under all operational wind scenarios [6–8]. Control strategies have to deal with unforeseen variables such as wind speed variability and intermittence, to achieve the goal of an overall acceptable performance. Various control techniques are used by researchers in the architecture of control strategies, amongst a wide variety of control types, some are mentioned here: Robust multivariable gain-scheduled control [9], fuzzy proportional integral [10], adaptive linear quadratic control [11], data-driven and adaptive PI control [12], sliding-mode control [13].

A suitable design for control and supervision under the unpredictable character of the wind energy is challenge in order to maximize power output. Thus, the controller needs to have access to the variables generator speed and pitch angle. The performance during the capture of wind energy is a prominent issue and has been dealt not only by research on turbine design and advanced control strategy, but also by condition monitoring using a supervisor. Some works addressed this issue, such

as: Classification of wind turbine condition monitoring methods and techniques with a focus on trends and future challenges [14], supervisory control and data acquisition system [15]. The supervisory control theory is behind the architecture proposed in this paper and is suitable for control application with event-based operations as can be seen in previous works [16,17].

This paper presents the following contributions: A two-level control architecture, consisting in a supervisory level (event-based supervisor) and an execution level (LQG and MPC controllers); a study and implementation of adaptive controllers and predictive controllers; a study of an event-based supervisor, having the objective of determining the most suitable operational state among the possible states; a simulation of the system with the distinct types of controllers with and without the presence of an event-based supervisor; and an evaluation of the system performance driven from the assessment of the results obtained with the action of each controller. In the overview of this paper, Section 2 presents the onshore energy conversion system modelling, Section 3 presents the control and supervision strategy applied to the system, namely the LQG, MPC in the execution level, an event-based supervisor in the supervision level and is also defined the operating regions according to the wind speed. Section 4 presents the simulation results as well the performance of the system without and with supervisor. Conclusions remarks are given in Section 5.

2. Onshore energy conversion system modelling

A mathematical model representing an appropriate and thorough dynamic of an onshore energy conversion system is developed in this section. The development of the mathematical model is based on the benchmark model developed in [19], whose electric power output is 4.8 MW. The proposed control and supervision hierarchical structure is represented by a block diagram model composed by the following functional systems: Mechanical system (blade-pitch angle and two-mass drive train), controllers (LQG and MPC), electrical system (generator and two-level converter) and event-based supervisor. The block diagram model shown in Figure 1, is composed by the following variables: v_w is the wind speed in m/s, τ_g and τ_r are the generator and turbine rotor torques in Nm, ω_g and ω_r are the generator and turbine rotor speed in rad/s, β_r is the pitch angle in degrees, P_g and P_r are the generator and reference power in MW. The r and m subscripts designate respectively reference and measurements values.

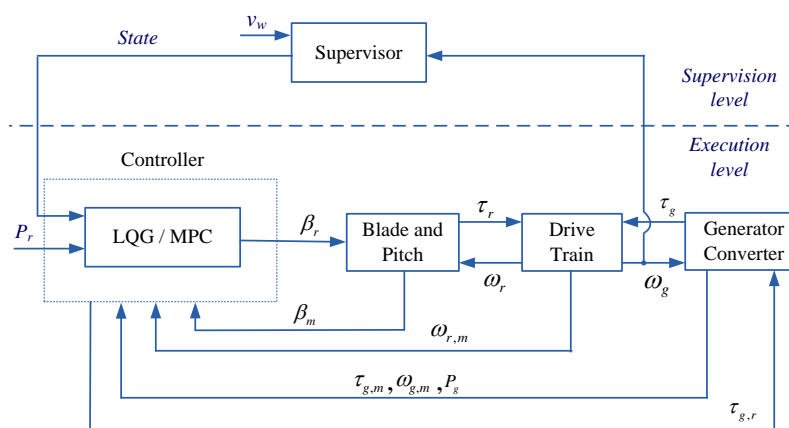


Figure 1. Proposed block diagram model.

2.1. Blade and pitch modelling

This model combines the aerodynamic with blade and pitch models. The aerodynamic torque is given by:

$$\tau_r(t) = \frac{\rho \pi R^3 C_p(\lambda(t), \beta(t)) v_w(t)^2}{2} \quad (1)$$

Where R is the radius of the blades, ρ is the air density, $C_p(\lambda(t), \beta(t))$ is the power coefficient, which is a function of the tip speed ratio $\lambda(t)$ and the pitch angle $\beta(t)$. The tip speed ratio is given by:

$$\lambda(t) = \frac{\omega_r(t)R}{v_w(t)} \quad (2)$$

From Eq 2, variations of the wind speed can lead to two consequences:

- If the turbine rotor speed is held constant, then $\lambda(t)$ will change, leading to a consequent change in the power coefficient;
- If the turbine rotor speed is suitably adjusted, then $\lambda(t)$ can be held at a reference point and as a result power coefficient can be kept at a desired value.

The power coefficient of a wind turbine using pitch control [20–23] is given by:

$$\begin{cases} C_p(\lambda, \beta) = 0.73 \left(\frac{151}{\lambda_i} - 0.58\beta - 0.002\beta^{2.14} - 13.2 \right) e^{\frac{-18.4}{\lambda_i}} \\ \lambda_i = \frac{1}{\frac{1}{(\lambda - 0.02\beta)} - \frac{0.003}{(\beta^3 + 1)}} \end{cases} \quad (3)$$

The pitch angle can be modelled as a second order differential equation given by:

$$\ddot{\beta}(t) = -2\xi\omega_n(t)\dot{\beta}(t) - \omega_n^2\beta(t) + \omega_n^2\beta_r(t) \quad (4)$$

2.2. Drive-train modelling

The mechanical drive train is composed by two shafts, a low-speed shaft from the rotor side, a high-speed shaft from the generator side, connected by a transmission equipped with a gear box. The two-mass drive train is shown in Figure 2.

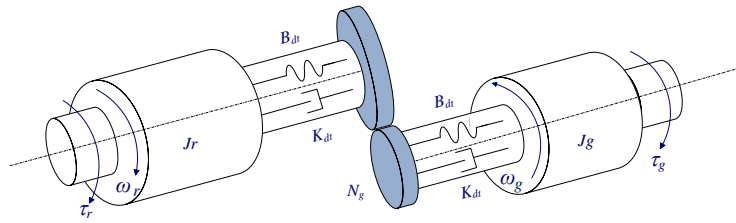


Figure 2. Two-mass drive train model.

The mathematical model to describe the dynamic of the drive train is a two-mass model. On the rotor side, the mass J_r concentrates the inertia of the hub, turbine blades and low-speed shaft inertia. On the generator side, J_g concentrates the generator inertia and high-speed shaft. The low-speed shaft and high-speed shaft are connected by a gear box with a ratio N_g . The torsion shaft stiffness is K_{dt} and torsion shaft damping is B_{dt} . The angular deviation due to the damping and stiffness coefficients between the turbine and the generator is $\theta_\Delta(t)$. The linear model for the drive train model is given by:

$$J_r \dot{\omega}_r(t) = \tau_r(t) + \frac{B_{dt}}{N_g} \omega_g(t) - K_{dt} \theta_\Delta(t) - (B_{dt} + B_r) \omega_r(t) \quad (5)$$

$$J_g \dot{\omega}_g(t) = \frac{K_{dt}}{N_g} \theta_\Delta(t) + \frac{B_{dt}}{N_g} \omega_r(t) - \left(\frac{B_{dt}}{N_g^2} + B_g\right) \omega_g(t) - \tau_g(t) \quad (6)$$

$$\dot{\theta}_\Delta(t) = \omega_r(t) - \frac{1}{N_g} \omega_g(t) \quad (7)$$

2.3. Generator and converter modelling

The model for the generator and the power converter is described by the state equation given by:

$$\dot{\tau}_g(t) = -\alpha_{gc} \tau_g(t) + \alpha_{gc} \tau_{g,r}(t) \quad (8)$$

Where α_{gc} is a first order constant and $\tau_{g,r}$ is the reference torque of the generator. The power of electric generator is given by:

$$P_g(t) = \eta_g \omega_g(t) \tau_g(t) \quad (9)$$

Where η_g is the efficiency of the generator.

3. Control and supervision strategy

The onshore energy conversion system components, the wind speed and the wind turbulence, the tip speed ratio and the pitch angle are some of the variables considered in the control design to achieve the rated power with an acceptable overall performance. In this paper two distinct controller are considered, adaptive and predictive. The control and supervision strategy are based on the switching from Region II (constant-pitch, generator torque control) to Region III (variable-pitch control, constant torque). Region II (wind speed is between 5 m/s and 13 m/s) and Region III (wind speed is between 14 m/s and 22.5 m/s) can be seen at the regions of power operation as shown in Figure 3.

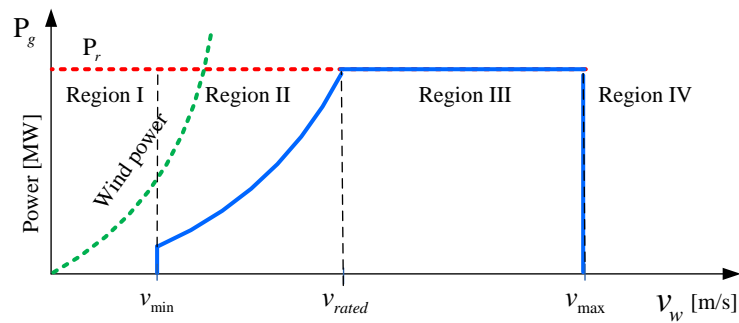


Figure 3. Operating regions of power [18].

Figure 3 shows that in Region II, the control objective is to extract optimal power reducing oscillation on the drive train, thus torque control is applied. The pitch angle and tip speed ratio are set to their optimal value to achieve this control objective and the rotor speed must be adjusted to the reference rotor speed given by:

$$\omega_{ref}(t) = \frac{\lambda_{opt}(t)v_w(t)}{R} \quad (10)$$

The optimal electric generator torque is given by:

$$\begin{cases} \tau_{g,r}(k) = K_{opt} \left(\frac{\omega_{ref}(k)}{N_g} \right)^2 \\ K_{opt} = \frac{1}{2} \rho A R^3 \frac{C_{p,max}}{\lambda_{opt}^3} \end{cases} \quad (11)$$

Where λ_{opt} is the optimal point for achieving maximum C_p and A is the area swept by the blades.

Figure 3 shows that in Region III, the control objective is to control the output generator power through pitch control. To achieve this control objective, the pitch angle varies according the error between nominal speed and the output generator speed. The pitch reference and generator torque reference should be adjusted at the same time and the latter is given by:

$$\tau_{g,r}(k) = \frac{P_r(k)}{\eta_g \omega_g(k)} \quad (12)$$

Switching between Region II and Region III is determined by the electric generator power, P_g , and the generator speed, ω_g , the control mode switching is performed according to the following conditions: Switching from Region II to Region III is enabled if $P_g > P_r$ and $\omega_g > \omega_{nom}$ and switching back from Region III to Region II is enable if $\omega_g < \omega_{nom} - \omega_\Delta$. The non-null threshold ω_Δ is required to enable preventing sudden switches from Region III and Region II.

3.1. Adaptive linear quadratic gaussian controller

Discrete adaptive linear quadratic gaussian control (LQG) deals with unpredicted variables and the adaptation depends on estimation of parameter $\hat{\theta}(k)$. Using recursive least squares algorithm, polynomials parameters from $A_l(z^{-1})$ and $B_l(z^{-1})$ can be estimated, obtaining parameters $\hat{\theta}(k) = [\hat{a}_{11} \hat{a}_{12} \hat{b}_{11} \hat{b}_{12}]$. The dynamic development of this controller is presented in [24]. The dynamical system of the onshore wind turbine benchmark around a nominal set-point $r(k)$ is represented by an ARX model, thus the linear quadratic control transfer function is given by:

$$\frac{Y(z)}{U(z)} = \frac{(b_{11}z^{-1} + b_{12}z^{-2})}{(1 + a_{11}z^{-1} + a_{12}z^{-2})} \quad (13)$$

Where the Z-transform of the system output and control input are respectively $Y(z)$ and $U(z)$. The performance index H is given by:

$$H(k) = (Py(k+d) - Qr(k))^2 + (\chi u(k))^2 \quad (14)$$

Where P and Q assume a unit value, the scalar $\chi = 0.4$ is chosen to achieve an acceptable closed-loop performance and optimal control $u(k)$ minimizes performance index.

The LQG pitch control structure is shown in Figure 4.

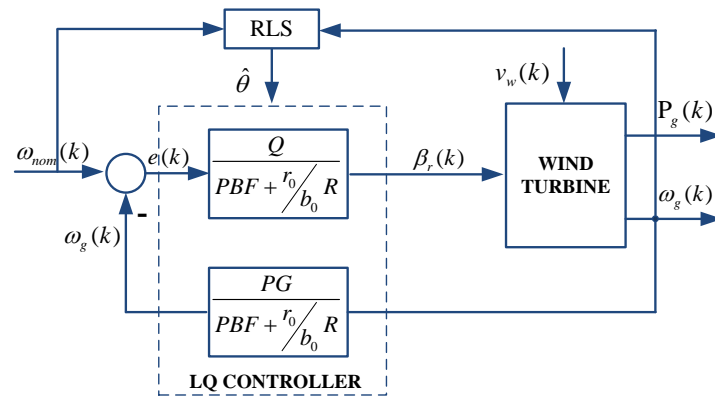


Figure 4. LQG pitch control structure.

The polynomials $F(z^{-1})$ and $G(z^{-1})$ can be determined by solving the Diophantine equation. The optimal control that minimizes the performance index is given by:

$$u(k) = \frac{\hat{b}_{11}}{\hat{b}_{11}^2 + \chi^2} \left[\left(\frac{\rho^2 - \hat{b}_{12} \hat{b}_{11}}{\hat{b}_{11}} \right) u(k-1) + \hat{a}_{11} y(k) + \hat{a}_{12} y(k-1) + r(k) \right] \quad (15)$$

3.2. Model predictive controller

Model predictive controller [25] use the states of the blades and pitch model, drive train and nonlinear aerodynamics as input. By optimizing the best output according to the operating region and control objective, the model predictive controller generates reference values for $\beta(k)$ and $\tau_{g,r}(k)$. From Eq 1 to Eq 9 a linear state space model representing the onshore energy conversion system dynamics at certain operating wind speed is given by:

$$\begin{cases} \mathbf{x}(k+1) = \mathbf{A}\mathbf{x}(k) + \mathbf{B}\mathbf{u}(k) \\ \mathbf{y}(k) = \mathbf{C}\mathbf{x}(k) \end{cases} \quad (16)$$

Where $\mathbf{x} = [\omega_r \ \omega_g \ \theta_\Delta \ \tau_g \ \beta]^T \in \mathbb{R}^5$ is the state vector, $\mathbf{u} = [\tau_{g,r} \ \beta_r]^T \in \mathbb{R}^2$ is the control input and $\mathbf{y} = [\omega_g \ P_g]^T \in \mathbb{R}^2$ is the measured output. One important purpose in this region is to maintain the generator speed very close to the nominal speed with the least stress on the generator and pitch control system. To accomplish this objective, one must follow the mathematical formulation for the objective function, i.e., the cost function is given by:

$$\min_{u(k) \dots u(k+Np-1)} J(k) = \underbrace{\sum_{j=1}^{Np} [r(k+j) - \hat{y}(k+j|k)]^T Q(j) [r(k+j) - \hat{y}(k+j|k)]}_{\text{Quadratic Error}} + \underbrace{\sum_{j=0}^{Np-1} [u(k+j|k)]^T R(j) [u(k+j|k)]}_{\text{Control Effort}} \quad (17)$$

In Eq 17 the cost function is associated with the prediction horizon, given by the periods j with $j = 1, \dots, Np$. The first term is a quadratic functional, weighted by matrix Q , of the difference

between reference $r(k+j)$ and predicted output $\hat{y}(k+j|k)$ and is used for penalization of the error. Also, the second term is a quadratic functional, weighted by matrix R , measuring the control effort $u(k+j|k)$.

The MPC pitch control structure is shown in Figure 5.

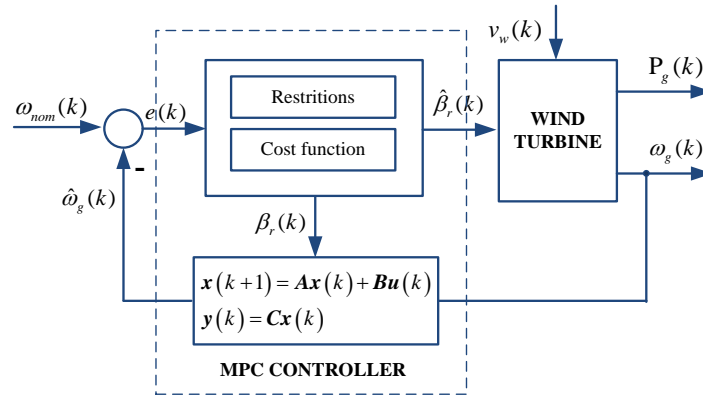


Figure 5. MPC pitch control structure.

The optimization problem consists in the minimization of the cost function subjected to the following constraints: $\beta_{\min} \leq \beta_r \leq \beta_{\max}$, $(\omega_{nom} - \omega_{\Delta}) \leq \omega_g \leq (\omega_{nom} + \omega_{\Delta})$ and also $v_{\min} \leq v_w \leq v_{\max}$.

Where ω_{nom} is the nominal generator speed and ω_{Δ} is a small offset that introduce some hysteresis in the switching scheme avoiding frequent switching from control modes.

3.3. Supervisor

The onshore energy conversion system event-based supervisor is based on finite state machine (FSM) also known by finite-state automaton or state machine. This machine is a mathematical model of computation to conveniently schedule the operational states of a process. The states are such as: start, production and stop. The machine is in only one state at a time and can change from one state to another when initiated by a triggering event or condition called a transition. The machine is a set of: behavior states, transitions that define the transit between states and rules or conditions to be fulfilled in order to enable a transition. The specification of a machine is given by the list of states and the triggering condition for transitions. The FSM is described by a quintuple model [26] given by:

$$FSM = (\Sigma, Q_f, \partial, q_0, Q_m) \quad (18)$$

In Eq 18 the Σ is the input alphabet, Q_f is the finite set of states, $\partial = \Sigma \times Q$ is the transition function, q_0 is the initial state and Q_m is the set of final states. The event-based supervisor deterministic

version of an FSM used in this paper has the state transition diagram shown by Figure 6.

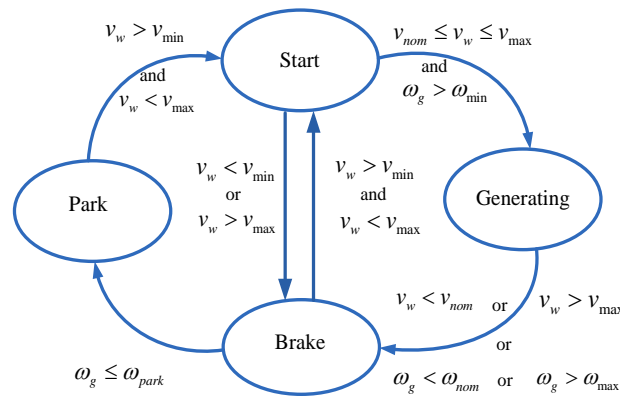


Figure 6. Supervisor.

In Figure 6, the operational states are park, start, generating and brake, typifying the regions of power operation as follow:

- In the Park state, the wind turbine is in shutdown mode and the generator is disconnected from the electric grid. This state corresponds to Region I.
- In the Start state, the wind speed must be above the cut-in speed (v_{min}). The wind turbine should be started to capture energy from the wind power. The generator is connected to the electric grid, but not necessarily at rated power in the majority of the operation in Region II. From this state and depending on the accuracy of the transitions (wind speed and generator speed), one can enter into the generating state or into the brake state. This state corresponds to Region II.
- In the Generating state, also known as power production, the wind speed must be within the rated wind speed (v_{rated}) and the cut-out speed (v_{max}). The generator is connected to the electric grid at rated power, by conveniently curtailment of the capture of kinetic energy from the wind. This state corresponds to Region III.
- In the Brake state, also known as slow down state, the pitch angle is adjusted in order to decrease the rotation of the wind turbine. From this state and according to the value of the conditions, one can enter into the start state or into the park state.

4. Results

The mathematical model of the WECS equipped with a two-level power converter topology is used in the simulations. The simulations in order to compare the performance without or with the supervisor are carried out in Matlab/Simulink. The time horizon considered in the simulations is of 4500 s, and the sampling time T_s is of 0.01 s. The WECS has a rated electric power of 4.8 MW for a wind speed v_w of 13 m/s, where ω_{nom} is 162 rad/s, ω_{Δ} is 15 rad/s and ω_{max} is 200 rad/s [19,27–29].

The series for the wind speed used in the simulations are the ones given in [19], having amplitudes in the range of 7.5 m/s to 22.5 m/s between Region II and Region III, but an addition of white noise to the wind speed is considered in order to have an augment effect of intermittence of wind energy. The

wind speed with the addition of white noise is shown in Figure 7.

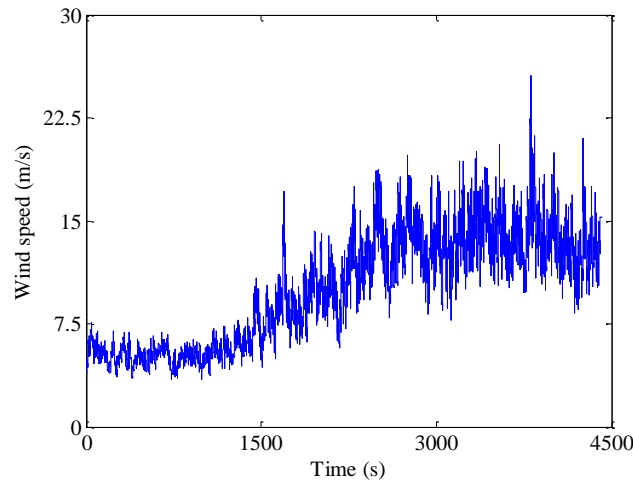


Figure 7. Wind speed with white noise.

4.1. Without supervisor

The following figures represent the simulations of the controllers, LQG and MPC, without the presence of the event-based supervisor. The electric output and reference power of the LQG and the MPC controllers are shown in Figures 8a, b.

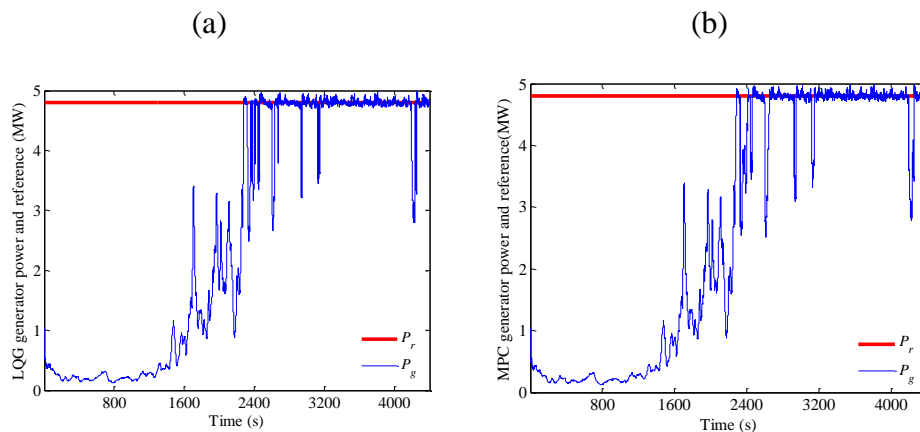


Figure 8. Electric and reference power: (a) LQG; (b) MPC.

In Figure 8 both controllers, the electric output power follows the reference power with some oscillations around the reference power having some decreases in the output power. Major strengths of MPC are abilities to handle multivariable interactions and operating constraints in systematic manner. MPC is formulated as a constrained optimization problem, which is solved on-line repeatedly by carrying out model-based forecasting over a moving window of time. More importantly, MPC facilitates optimal control systems with unequal number of manipulated inputs and measured outputs. LQG provides a systematic approach to designing a control law for linear

multi-variable systems. However, some difficulties associated with the classical LQG formulation is inability to handle operating constraints explicitly. Operating constraints, such as limits on manipulated inputs or on their rates of change, limits on controlled outputs arising out of product quality or safety considerations, are commonly encountered in any control application.

MPC can be viewed as modified versions of LQ (or LQG) formulation, which can deal with the operating constraints in a systematic manner. Origins of MPC can be traced to the classical linear quadratic optimal control (LQOC) formulation. These techniques, although have different mechanisms, are similar, thus, giving similar outputs.

The LQG controller and the MPC controller pitch angles are shown in Figures 9a, b.

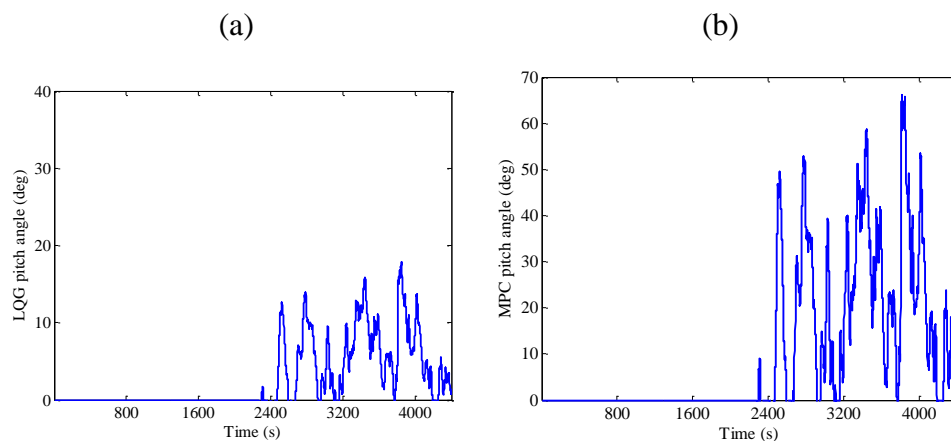


Figure 9. Pitch angle: (a) LQG; (b) MPC.

In Figure 9 LQG controller provides pitch angle variations between 7 degrees and 18 degrees. MPC controller provides pitch angle variations between 10 degrees and 65 degrees.

The switching between Region II and Region III is shown in Figures 10a, b.

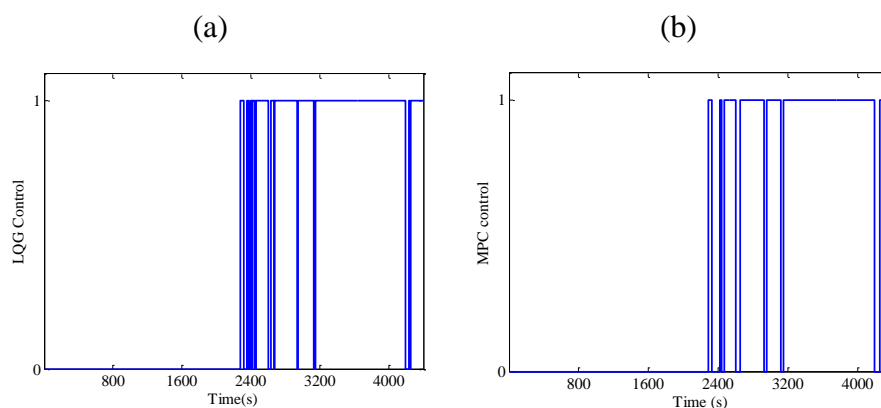


Figure 10. Control switching: (a) LQG; (b) MPC.

In Figure 10 Region II (0) corresponds to startup operational mode and Region III (1) corresponds to generation operational mode. Both controllers present, with some frequency, switching between Region II and Region III.

4.2. With supervisor

The following figures represent the simulations of the controllers, LQG and MPC, with the presence of the event-based supervisor. The electric output and reference power of LQG and the MPC controllers are shown in Figures 11a, b.

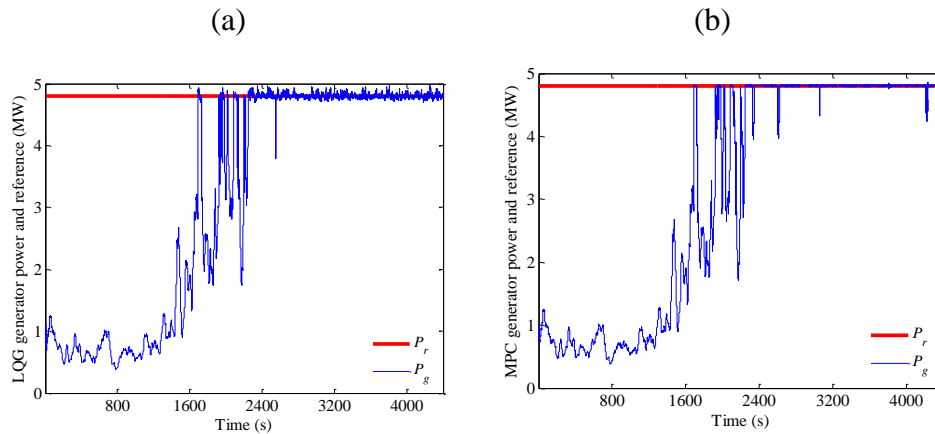


Figure 11. Electric and reference power: (a) LQG; (b) MPC.

In Figure 11 MPC controller allows a smoother response around reference power, when compared to the one obtained with the LQG controller, however presents several peaks.

The LQG controller and the MPC controller pitch angles are shown in Figures 12a, b.

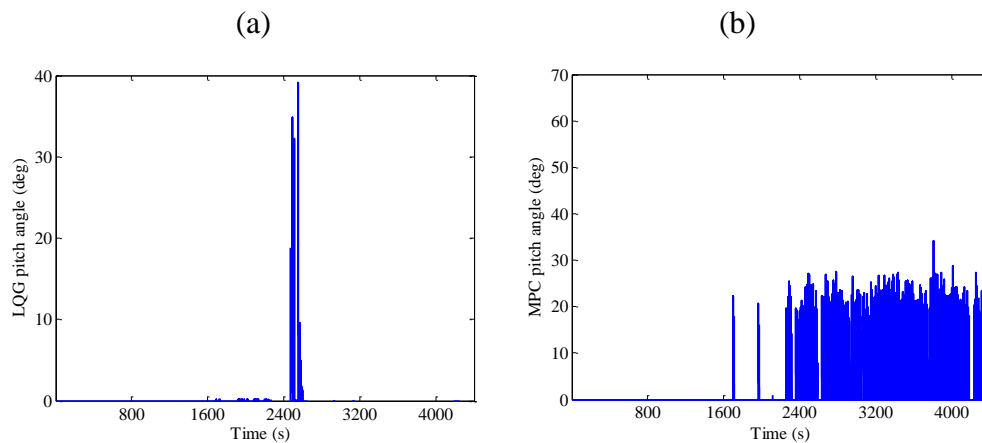


Figure 12. Pitch angle: (a) LQG; (b) MPC.

In Figure 12 LQG controller pitch angle variation only occurs in a small interval of time reaching the maximum of 40 degrees. LQG controller contributes to less variation on the pitch angle. MPC controller provides pitch angle variations between 15 degrees and 25 degrees having one peak above 30 degrees.

The switching between Region II and Region III is shown in Figures 13a, b.

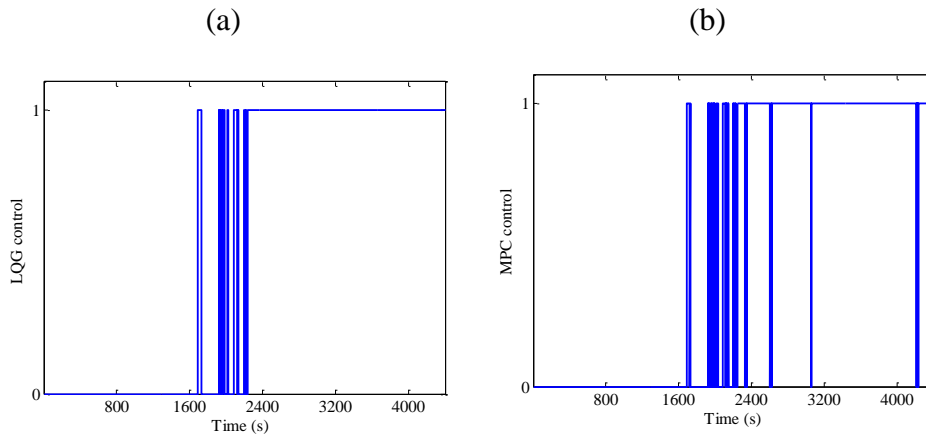


Figure 13. Control switching: (a) LQG; (b) MPC.

In Figure 13 the transition between the two operational states is due to the need of sustaining the electric output at the rated power. The LQG controller allows a less frequent switching between Region II and Region III, with permanence in Region III while MPC controller presents few switching between Region II and Region III.

4.3. Performance assessment

The metrics used in the evaluation of the performance of the controller are the integral of time multiplied by the absolute value of the error (ITAE) and the integral of the square value (ISV). The ITAE is given by:

$$ITAE = \int_0^{t_f} t |e(t)| dt \quad (19)$$

And the ISV is given by:

$$ISV = \int_0^{t_f} u^2(t) dt \quad (20)$$

The control performances for the WECS without or with supervisor control are summarized in Table 1.

Table 1. Performance assessment results.

Controller	LQG	MPC
Without Supervisor		
ITAE	1.0792×10^{15}	1.0886×10^{15}
ISV	1.0770×10^7	1.4791×10^7
With Supervisor		
ITAE	7.0328×10^{14}	7.0250×10^{14}
ISV	2.7171×10^5	1.7276×10^7

In Table 1 considering the values obtained without the event-based supervisor, the error between

the electrical output and the reference power is smaller with the LQG controller, although with the MPC the error is close to that presented by the LQG controller. As far as the control effort is concerned, the LQG controller has a smaller error when compared to the MPC controller, consuming less energy. Considering the values obtained under the event-based supervisor, both controllers accomplish equivalent performance with respect to the error between electric output and reference power. Regarding the control action effort, it is observed that the lowest effort is obtained with the LQG controller while the MPC requires more energy to maintain the output power around reference power.

5. Conclusion

An onshore energy conversion system connected to the electric grid and under an event-based supervisor control is presented. The control and supervision strategy proposed for the onshore energy conversion system is based on a hierarchical structure with two levels. LQG and MPC controllers are in the execution level whereas the event-based supervisor is placed in the supervision level.

The closed loop response between LQG and MPC without supervisor is quite similar, with abrupt variations around reference power. The pitch angle variations achieve lower amplitude values with the LQG controller. In terms of performance, LQG controller outperforms the latter at expense of lower control effort.

The closed loop response with supervisor remains similar as the above one, with smoother variations around reference power. The pitch angle variations with LQG only occurs in a small interval of time reaching the maximum of 40 degrees. In terms of performance, LQG controller maintains superiority over MPC.

Acknowledgments

This work is funded by: European Union through the European Regional Development Fund, included in the COMPETE 2020 (Operational Program Competitiveness and Internationalization) through the ICT project (UID/GEO/04683/2013) with the reference POCI010145FEDER007690; Portuguese Funds through the Foundation for Science and Technology-FCT under the project LAETA, reference UID/EMS/50022/2013; Portuguese Foundation for Science and Technology (FCT) under Project UID/EEA/04131/2013.

Conflict of interest

All authors declare no conflicts of interest in this paper.

References

1. World Wind Energy Association (2018) *Wind Power Capacity reaches 539 GW, 52,6 GW added in 2017*. Available from: <http://www.wwindea.org/2017-statistics/>
2. Vidal Y, Acho L, Luo N, et al. (2012) Power control design for variable-speed wind turbines. *Energies* 5: 3033–3050.
3. Garcia-Sanz M (2012) *Wind Energy Systems: Control Engineering Design*. CRC Press.

4. Melicio R, Mendes VMF (2005) Doubly fed induction generator systems for variable speed wind turbine. *In Proc. 9th Spanish-Portuguese Congress on Electrical Engineering-9CHLIE*, Marbella, Spain, 161–164.
5. Siraj K, Siraj H, Nasir M (2014) Modeling and control of a doubly fed induction generator for grid integrated wind turbine. *In IEEE International Power Electronics and Motion Control Conference and Exposition-PEMC 2014*, Antalya, Turkey, 901–906.
6. Zhang J, Cheng M, Chen, Z, et al. (2008) Pitch angle control for variable speed wind turbines. *In 3rd International Conference on Electric Utility Deregulation and Restructuring and Power Technologies-DRPT 2008*, Nanjing, 2691–2696.
7. Merabet A, Thongam J, Gu J (2011) Torque and pitch angle control for variable speed wind turbines in all operating regimes. *In 10th International Conference on Environment and Electrical Engineering-EEEIC 2011*, Rome, Italy, 1–5.
8. Lupu L, Boukhezzar B, Siguerdidjane H (2006) Pitch and torque control strategy for variable speed wind turbines. *In European Wind Energy Conference & Exhibition-EWEC 2006*, Athens, Greece, 1–7.
9. Bianchi FD, Battista HD, Mantz RJ (2010) Robust multivariable gain-scheduled control of wind turbines for variable power production. *Int J Syst Control* 1: 103–112.
10. Aissaoui AG, Tahour A, Essounbouli N, et al. (2013) A fuzzy-pi control to extract an optimal power from wind turbine. *Energ Convers Manage* 65: 688–696.
11. Mateescu R, Pinteau A, Stefanoiu D (2012) Discrete-time LQG control with disturbance rejection for variable speed wind turbines. *In 1st International Conference on Systems and Computer Science—ICSCS 2012*, Lille, France, 1–6.
12. Simani S, Castaldi P (2013) Data-driven and adaptive control applications to a wind turbine benchmark model. *Control Eng Pract* 21: 1678–1693.
13. Beltran B, Ahmed-Ali T, Benbouzid MEH (2008) Sliding mode power control of variable-speed wind energy conversion systems. *IEEE T Energy Convers* 23: 551–558.
14. Tchakoua P, Wamkeue R, Ouhrouche M, et al. (2014) Wind turbine condition monitoring: State-of-the-art review. *Energies* 7: 2595–2630.
15. Yang W, Jiang J (2011) Wind turbine condition monitoring and reliability analysis by SCADA information. *In IEEE International Conference on Mechanic Automation and Control Engineering—MACE 2011*, Hohhot, China, 1872–1875.
16. Qi W, Liu J, Chen X, et al. (2011) Supervisory predictive control of standalone wind/solar energy generation systems. *IEEE T Contr Syst T* 19: 199–207.
17. Sarrias R, Fernández LM, García CA, et al. (2011) Supervisory control system for DFIG wind turbine with energy storage system based on battery. *In: International Conference on Power Engineering, Energy and Electrical Drives-POWERENG*, Malaga, Spain, 1–6.
18. Johnson KE, Pao LY, Balas MJ, et al. (2006) Control of variable-speed wind turbines: Standard and adaptive techniques for maximizing energy capture. *IEEE Control Syst* 26: 70–81.
19. Odgaard PF, Stroustrup J, Kinnaert M (2013) Fault tolerant control of wind turbines: A benchmark model. *IEEE T Contr Syst T* 12: 1168–1182.
20. Melicio R, Mendes VMF, Catalão JPS (2010) Wind turbines equipped with fractional-order controllers: Stress on the mechanical drive train due to a converter control malfunction. *Wind Energy* 14: 13–25.

21. Melicio R, Mendes VMF, Catalão JPS (2008) Two-level and multilevel converters for wind energy systems: A comparative study. *In Proc. 13th International Power Electronics and Motion Control Conference-EPE-PEMC 2008, Poznań, Poland*, 1682–1687.
22. Melicio R, Mendes VMF, Catalão JPS (2010) Modeling, control and simulation of full-power converter wind turbines equipped with permanent magnet synchronous generator. *Int Rev Electr Eng-I 5*: 397–408.
23. Melicio R, Mendes VMF, Catalão JPS (2009) Modeling and simulation of wind energy systems with matrix and multilevel power converters. *IEEE Lat Am T 7*: 78–84.
24. William L (2010) *The Control Handbook*, 2nd ed., Florida: CRC Press.
25. Maciejowski JM, Goulart PJ, Kerrigan EC (2007) Constrained Control Using Model Predictive Control, *In: Tarbouriech S, Garcia G, Glattfelder AH (eds), LNICS, Springer, Heidelberg*, 346: 273–291.
26. Cassandras CG, Lafortune S (2000) Introduction to discrete event systems. Springer Science Business Media, New York, USA.
27. Viveiros C, Melicio R, Igreja JM, et al. (2015) Supervisory control of a variable speed wind turbine with doubly fed induction generator. *Energ Rep 1*: 89–95.
28. Viveiros C, Melicio R, Igreja JM, et al. (2015) Performance assessment of a wind energy conversion system using a hierarchical controller structure. *Energ Convers Manage 93*: 40–48.
29. Viveiros C, Melicio R, Igreja JM, et al. (2013) Application of a discrete adaptive LQG and fuzzy control design to a wind turbine benchmark model. *In Proc. 2nd International Conference on Renewable Energy Research and Applications-ICRERA 2013, Madrid, Spain*, 488–493.



AIMS Press

© 2018 the Author(s), licensee AIMS Press. This is an open access article distributed under the terms of the Creative Commons Attribution License (<http://creativecommons.org/licenses/by/4.0>)